Energy-Energy Correlator for Jet Production in *pp* and *pA* Collisions

João Barata,[1,*] Zhong-Bo Kang,[2,3,4,†] Xoán Mayo López,[5,‡] and Jani Penttala[2,3,§]

[1]*CERN, Theoretical Physics Department, CH-1211, Geneva 23, Switzerland*

[2]*Department of Physics and Astronomy, University of California, Los Angeles, California 90095, USA*

[3]*Mani L. Bhaumik Institute for Theoretical Physics, University of California, Los Angeles, California 90095, USA*

[4]*Center for Frontiers in Nuclear Science, Stony Brook University, Stony Brook, New York 11794, USA*

[5]*Instituto Galego de Física de Altas Enerxías, Universidade de Santiago de Compostela, Santiago de Compostela 15782, Galicia, Spain*

(Received 26 November 2024; revised 22 April 2025; accepted 2 June 2025; published 24 June 2025)

In this Letter, we study the collinear limit of the energy-energy correlator in single-inclusive jet production in proton-proton and proton-nucleus collisions. We introduce a nonperturbative model that allows us to describe the energy-energy correlator in the entire angular region of the current experiments. Our results for proton-proton collisions show excellent agreement with CMS and ALICE data over a wide range of jet transverse momenta. For proton-nucleus collisions, we include modifications from the nuclear medium, and our predictions align well with the trends observed in recent ALICE measurements.

DOI: 10.1103/96xh-bd1w

Introduction—Hadronic jets—energetic, collimated cascades of QCD particles produced in high-energy scattering experiments—are among the most powerful tools for probing the nature and properties of QCD. In events with low final-state particle multiplicity, such as those typically observed in electron-electron and proton-proton (pp) collisions, jets enable precise tests of the soft and collinear dynamics of QCD; see, e.g., [1–3]. In contrast, in collisional systems such as electron-nucleus, proton-nucleus (pA), and nucleus-nucleus (AA), the jet radiative cascade gets modified by the underlying QCD medium, whether it be the cold nuclear matter characterized by a highly occupied gluonic state [4,5] or the hot quark-gluon plasma [6]. By comparing these modified jets to those produced in electron-electron or pp collisions, one can investigate the medium-induced imprints on the jet cascade, providing a unique window into the many-body properties of QCD.

One of the key challenges in describing the vacuum fragmentation pattern of jets and extracting medium-induced modifications to jets lies in identifying observables that allow for both a theoretically consistent description and experimental accessibility across a broad kinematic region. Recently, it has been argued that correlations between asymptotic fluxes of certain currents can satisfy these requirements; see, e.g., [7–17]. Focusing on the widely studied case of energy-energy correlators (EECs) [18–21], in vacuum they allow, for example, to directly access the anomalous scaling of leading-twist QCD operators at high precision [8,9,20,22] and cleanly separate the relevant scales inside jets, sharply splitting perturbatively and nonperturbatively dominated sectors [8,17,22]. Extending this program to electron-nucleus, pA, and AA collisions, EECs have the potential to directly probe the scales of the underlying matter and resolve its spatial structure [12,23–35].

Despite this promise, the theoretical control of EECs in complex collisional systems, particularly AA collisions, remains limited. Current studies are mostly constrained to (partial) leading-order perturbative calculations [24,25,36] and numerical model simulations [25,34]. Even in cleaner environments such as electron-proton or pp collisions, the description of EECs in the nonperturbative sector is still poorly understood.

This nonperturbative region of EECs has recently garnered much interest due to the emergent scaling behavior, which is indicative of the hadronization transition's universality [15–17,22,37]. In the back-to-back limit of EECs where the transverse-momentum-dependent (TMD) factorization is valid, the nonperturbative region can be described using nonperturbative Sudakov factors related to the transverse momentum dependence of fragmentation, and the nonperturbative kernel required for a resummation of large logarithms in rapidity [11,38–41]. In the collinear limit, the Collins-Soper resummation is not needed, but the physics related to the nonperturbative fragmentation is expected to remain the same; see, e.g., [42]. Exploring the universality of these nonperturbative effects is then of high

*Contact author: joao.lourenco.henriques.barata@cern.ch

†Contact author: zkang@physics.ucla.edu

‡Contact author: xoan.mayo.lopez@usc.es

§Contact author: janipenttala@physics.ucla.edu

Published by the American Physical Society under the terms of the Creative Commons Attribution 4.0 International license. Further distribution of this work must maintain attribution to the author(s) and the published article's title, journal citation, and DOI. Funded by SCOAP³.

interest due to its potential in describing a vast range of observables across different experimental environments.

To develop a comprehensive understanding of jet substructure and medium-induced modifications from EECs, it is essential to have theoretical predictions that encompass both the perturbative and the nonperturbative sectors of pp collisions, while also incorporating medium-induced modifications for systems interpolating between pp and AA events. A prime candidate for this is pA collisions where high-energy jets can still be produced and fragment in the presence of cold nuclear matter [43–51]. This constitutes a *cleaner* environment when compared to the quark-gluon plasma, allowing us to directly probe the medium-induced modifications to EECs inside jets.

In this Letter, we present a formalism to describe the collinear limit of the EEC distribution in pp and pA collisions. Our framework accounts, at the same time, for both the nonperturbative regime, where a parametrization inspired by TMD factorization is implemented [11,52], and the perturbative sector, where we employ the leading-logarithmic (LL) evolution of the vacuum cascade as well as the medium-induced modifications to the partonic branchings in pA events. This holistic approach allows for an efficient description of the entire EEC region and can be extended to other collisional systems. As we shall show, this permits a first direct observation of purely medium-induced modifications to the jet cascade in pA collisions using EECs.

Proton-proton collisions—The collinear limit of the EEC distribution satisfies the factorization formula [8,9]

$$\frac{\mathrm{d}\Sigma^{pp}}{\mathrm{d}p_T \mathrm{d}y\,\mathrm{d}R_L} = \int_0^1 \mathrm{d}x\, x^2 \frac{\mathrm{d}J(x, p_T, R_L)}{\mathrm{d}R_L} \cdot H(x, y, p_T), \quad (1)$$

where we made implicit the dependence on the factorization scale μ, y denotes the rapidity, and p_T is the transverse momentum of the jet. This factorization formula separates the production of the outgoing states into a hard function H, which does not depend on the angular separation between the outgoing states R_L, and an EEC jet function J, which incorporates the collinear fragmentation inside the jet. Restraining our discussion to the LL accuracy, the convolution in Eq. (1) trivializes to setting $x = 1$, and the dot product is taken in flavor space, i.e., $J = \{J_q, J_g\}$, and $H = \{H_q, H_g\}$.

The hard function can be obtained from collinear factorization [53–56], where the cross section to extract a parton c from the initial hard scattering reads

$$\frac{\mathrm{d}\sigma_c}{\mathrm{d}p_T\,\mathrm{d}y} = \sum_{a,b} f_{a/p}(x_a, \mu) \otimes f_{b/p}(x_b, \mu) \otimes \hat{\sigma}_{a+b\to c}. \quad (2)$$

Here, $\otimes$ denotes a convolution over the parton momentum fraction, $\hat{\sigma}_{ab\to c}$ is the hard partonic cross section to produce a parton c with a transverse momentum p_T and rapidity y, and $f_{a/p}$ is the parton distribution function (PDF) associated to the parton a coming from the proton. The hard function can then be defined from Eq. (2) as $H(y, p_T, \mu) = \{\mathrm{d}\sigma_q/(\sigma \mathrm{d}p_T\,\mathrm{d}y), \mathrm{d}\sigma_g/(\sigma \mathrm{d}p_T\,\mathrm{d}y)\}$ [57–60], which is normalized by the jet cross section σ as in the definition of the EEC. We choose the factorization scale $\mu = p_T$ for the central predictions shown in the plots below.

Moving to the jet function, we first note that renormalization group consistency implies that, at the LL accuracy, J satisfies a multiplicative renormalization formula, which results in the differential jet function [9]

$$\frac{\mathrm{d}J}{\mathrm{d}R_L} = \frac{\alpha_s(R_L p_T)}{\pi R_L}(1,1) \cdot \left(\frac{\alpha_s(\mu)}{\alpha_s(R_L p_T)}\right)^{\frac{\gamma(3)}{\beta_0}} \cdot \gamma(3), \quad (3)$$

where $\beta_0 = (11C_A - 2n_f)/3$ and $\gamma(j) \equiv -\int_0^1 \mathrm{d}z\, z^{j-1}\hat{P}(z)$ is the anomalous dimension matrix, with $\hat{P}$ being the regularized splitting function, such that only the spin $j = 3$ contributes to the EEC at the leading power. As a result, Eq. (3) defines the perturbative vacuum component of the EEC jet function.

So far, we have discussed the perturbative sector where $R_L p_T \gg \Lambda_{\mathrm{QCD}}$. At lower scales, the EEC becomes highly sensitive to nonperturbative dynamics in the fragmentation process. The underlying physics of fragmentation leading to the modification of the momentum distribution should be the same as in the back-to-back limit, and thus we model it using a form inspired by the nonperturbative Sudakov factor in TMD factorization [11,42],

$$j_{\mathrm{np}}(b) = \exp(-a_0 b), \quad (4)$$

where a_0 is a *free* parameter accounting for nonperturbative effects. We note that the parameter a_0 should differ for quarks and gluons due to their different color charge, but in this Letter we shall not consider the separation in flavor. In the momentum space, we can interpret j_{np} as a probability distribution for the produced hadrons to get additional transverse momentum in the fragmentation, and the condition $j_{\mathrm{np}}(b = 0) = 1$ guarantees that the distribution is correctly normalized. Furthermore, we note that this nonperturbative element inherits the universal behavior of the hadronization transition and can thus be applied to extractions of the (vacuum) jet EEC in other processes; we discuss the medium-induced modifications below. To incorporate this nonperturbative element, it is convenient to work in the position space where the convolution is multiplicative,

$$\frac{\mathrm{d}\Sigma^{pp}}{\mathrm{d}p_T \mathrm{d}y\,\mathrm{d}R_L} = R_L p_T^2 \int_0^\infty \mathrm{d}b\, b J_0(R_L p_T b) j_{\mathrm{np}}(b) \tilde{\Sigma}(b), \quad (5)$$

$$\tilde{\Sigma}(b) = (1,1) \cdot \left(\frac{\alpha_s(R p_T)}{\alpha_s(\mu_{b_*})}\right)^{\frac{\gamma(3)}{\beta_0}} \cdot H. \quad (6)$$

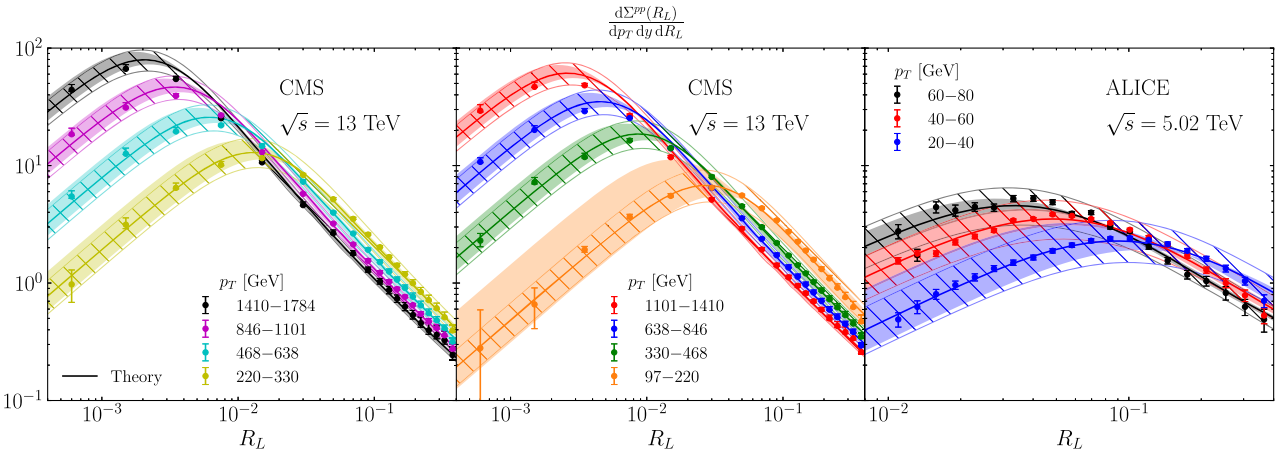


FIG. 1. Differential EEC distribution in pp collisions as a function of the angle R_L compared to the experimental data from CMS [16] and ALICE [17]. The theory prediction at the average p_T of the bin is shown with solid lines, while the shaded band corresponds to the prediction with the minimum and maximum p_T in each bin. The hatched bands indicate the theoretical uncertainty associated with resummation scale variation, obtained by independently varying the scales $\mu_{b_\star}$ in Eq. (6) and μ in Eq. (2) up and down by a factor of 2, and taking the envelope of the resulting predictions.

This relation follows from evolving the jet function in the position space where the initial scale $R_L p_T$ is replaced by $\mu_{b_*} = 2e^{-\gamma_E}/b_*$; see Supplemental Material [61]. This choice minimizes large logarithms that appear at higher orders, and we use the standard b_* prescription $b_* = b/\sqrt{1 + b^2/b_{\max}^2}$ with $b_{\max} = 2e^{-\gamma_E}\ \mathrm{GeV}^{-1}$ [62,63]. Equation (5) resums the same logarithms as the momentum-space expression in Eq. (3). We take into account the finite jet radius $R = 0.4$, consistent with the experimental data, by evolving the jet function up to Rp_T [64].

The numerical results for the EEC in pp collisions are shown in Fig. 1, with the parameter a_0 characterizing nonperturbative physics chosen as $a_0 = 3.8$ GeV for CMS and $a_0 = 2.5$ GeV for ALICE, fitted to the experimental data presented in [16] and [17], respectively. We use the CT18ANLO fit [65] for the proton PDF, and we also incorporate a K factor of $K \approx 0.90$ for CMS and $K \approx 0.75$ for ALICE to account for higher-order corrections beyond the LL approximation in our formalism. The difference in a_0 arises from the experimental definitions of jet p_T [66]: ALICE reports charged jets, where p_T is the sum over charged particles only, while CMS uses inclusive jets, summing over both charged and neutral particles. Assuming isospin symmetry, rescaling the ALICE value by a factor of $3/2$ yields $a_0 \approx 3.75$ GeV, consistent with the CMS value. This consistency highlights the robustness of our model across different jet definitions and kinematic regimes.

A direct analysis of Fig. 1 allows us to conclude that our description, accommodating the LL perturbative prediction at large angles and a nonperturbative jet function at small angles, can describe the data quite precisely in the entire angular domain and for a wide range of different p_T values. We note that while the large-angle region is fully determined from perturbative considerations, the nonperturbative sector for all of the curves in each experiment is described by the same a_0 parameter, in agreement with the universal character of j_{np}. Most crucially, we capture the location of the distribution's peak for all values of p_T, indicating a good theoretical description of the transition between the two sectors.

Proton-nucleus collisions—Having introduced a description of the EEC in pp collisions in the full angular domain, we extend our construction to collisional systems where a QCD background medium is present. The presence of the medium can, in general, induce modifications to both the hard and the EEC jet functions. In pA collisions, the hard function should be updated to account for the target nucleus. To that end we replace one of the PDFs in Eq. (2) by a nuclear PDF (nPDF), i.e., $f_{b/p}(x_b, \mu) \to f_{b/A}(x_b, \mu)$.

The jet function receives medium-induced modifications to the perturbative and nonperturbative sectors. For the former, the medium correction enters as a higher-twist or power correction to the leading perturbative QCD result. Thus, it cannot change the renormalization group evolution at the current accuracy, and the corrections can be entirely incorporated into the fixed-order jet function that now reads $J^{pA} = J^{pp} + J^{\mathrm{med}}$, with

$$\frac{\mathrm{d}J^{\mathrm{med}}}{\mathrm{d}R_L} = \frac{\alpha_s(R_L p_T)}{\pi R_L} \int_0^1 \mathrm{d}x\, x(1-x) P^{\mathrm{vac}}(x) F_{\mathrm{med}}(p_T, R_L, x), \tag{7}$$

where the medium modification (matrix) factor F_{med} depends on the jet quenching parameter $\hat{q}$ and the effective path length in the medium L. Here P^{vac} denotes the appropriate vacuum splitting kernel. In the large-N_c limit, F_{med} can be explicitly computed in a semiclassical

expansion [67,68]; we provide the explicit formulas in Supplemental Material [61] (see also Refs. [67–73] therein).

The nonperturbative sector of J^{pA} is also modified compared to pp collisions. Physically, these corrections are driven by the multiple scattering of the jet partons on the nucleus, which results in the broadening of the underlying momentum distribution. Thus, at small angles we update Eq. (4) to the form

$$j_{\rm np}(b) = \exp(-a_0 b - a_1 b^2), \tag{8}$$

where a_0 is the same as in the vacuum case and the parameter a_1 accounts for the medium-induced diffusive contribution to the hadronization of the jet partons. Note that a_1 captures the relative transverse momentum broadening of a particle pair inside the jet, differing, in general, from the standard $\hat{q}L$ scaling for a single parton. Finally, we also note that, as in AA collisions, one should account for energy-loss effects that can affect the nonperturbative sector. However, since in pA collisions these are expected to be negligible due to the smallness of $\hat{q}$ and L, we shall neglect them in what follows.

We consider a typical value for the jet quenching parameter in cold nuclear matter, $\hat{q} = 0.02\ \mathrm{GeV}^2/\mathrm{fm}$ [74,75], and take the path length to be $L = 3$ fm, while the nonperturbative medium-dependent parameter is set at $a_1 = 0.25\ \mathrm{GeV}^2$. The K factors, the proton PDF, and the a_0 parameter are the same as in our pp analysis, while we use the EPPS21 fit [76] for the nPDF.

The numerical results for the ratio between the differential EEC in p Pb with respect to pp collisions as a function of the opening angle, defined as $R_{pA} = [\mathrm{d}\Sigma^{pA}(R_L)/\mathrm{d}p_T\,\mathrm{d}y\,\mathrm{d}R_L]/[\mathrm{d}\Sigma^{pp}(R_L)/\mathrm{d}p_T\,\mathrm{d}y\,\mathrm{d}R_L]$, are shown in Fig. 2, along with the fit to the experimental data in the $p_T \in (20, 40)$ GeV bin provided by the ALICE Collaboration [77] (dot-dashed black line). We first note that the effect of the nPDF (dashed green line) is almost negligible for the whole R_L range. This is expected since the EEC is normalized by the jet cross section, and the effect of nPDF mostly cancels out in the ratio. We then present two predictions, one including only the medium modification to the nonperturbative sector (dotted red line) and one including all the medium effects (solid blue line). As is evident when comparing to the experimental fit, our modification to $j_{\rm np}$ is crucial to capture the data trend for a suppression in R_{pA}. This gives a clear indication of the importance of momentum broadening in the nucleus at small transverse momentum scales. We note that, so far and to our best knowledge, momentum diffusion had only been taken into account in the perturbative region of the EEC.

Comparing the experimental fit to the theory at large R_L, we clearly observe the enhancement effect driven by the medium modification factor $F_{\rm med}$. Note that at small angles $F_{\rm med} \approx 0$, and thus it does not affect the nonperturbative region. Moreover, compared to the case of AA collisions

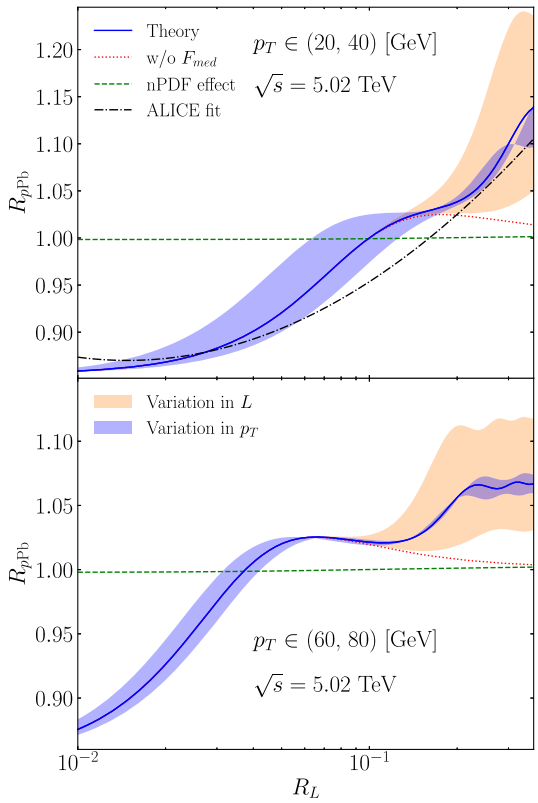


FIG. 2. Ratio of the differential EEC pPb distribution with respect to pp collisions, as a function of R_L, compared to the experimental fit provided by ALICE [77] (dot-dashed black line): $R_{p\mathrm{Pb}}^{\mathrm{ALICE}} = 0.87 + 0.121[\log_{10}(R_L) + 1.831]^2$. The theory prediction, at the average p_T of the bin, is shown by the blue solid line. The ratio with $F_{\rm med} = 0$ (dotted red line), and the sole effect of introducing the nPDF in the vacuum distribution (dashed green line) are also shown. The blue shaded band corresponds to the prediction using the minimum and maximum p_T of the bin, while the orange band corresponds to modifying the length of the medium $L \in (2, 4)$ fm.

where there is a competing effect driven by the soft physics of the bulk [25,34,78], in the pA scenario the medium does not significantly contaminate the jet. As a result, our analysis provides first evidence for the emergence of medium-induced jet modifications in the EEC distribution, within a simple and improvable theoretical model. We further note that the approximations used to compute $F_{\rm med}$ in this work tend to overestimate the enhancement, and thus improved theoretical descriptions would most likely drive the model curve closer to the experimental fit; see discussion in [24]. We also provide a prediction for jets with $p_T \in (60, 80)$ GeV in the lower panel of Fig. 2 to illustrate the p_T dependence of the nuclear modification.

Conclusions—In this Letter, we have presented a theoretical framework for the differential EEC distribution in the collinear limit, encompassing both pp and pA collisions. Our model incorporates the leading-logarithmic form of the observable in the perturbative sector and employs a

TMD-inspired parametrization to describe the nonperturbative regime. By fitting the available CMS and ALICE pp data, we have achieved excellent agreement with experiment, successfully describing the EEC at both small and large angles and accurately predicting the location of the distribution's peak. For pA collisions, our formalism incorporates nuclear medium effects, enabling a unified description across both the nonperturbative and the perturbative regions.

In the small-angle region, we have highlighted the critical role played by medium-induced broadening, essential to accurately capture the hadronization transition. At large angles, we have included the leading medium-induced power corrections, demonstrating that these lead to a significant enhancement compared to pp data. Contrasting our theoretical predictions with ALICE's fit to experimental data [77], we have shown that our framework provides a precise and comprehensive description of the measurements.

This work establishes a solid foundation for a future detailed and thorough understanding of the jet EEC across a diverse set of experiments, opening exciting opportunities for future research.

Acknowledgments—We thank B. Jacak and A. Nambrath for their valuable discussions regarding the ALICE measurements. X. M. L. thanks the nuclear physics group at UCLA for their hospitality during the development of this work. Z. K. and J. P. are supported by the National Science Foundation under Grant No. PHY-1945471. The work of X. M. L. is supported by European Research Council project ERC-2018-ADG-835105 YoctoLHC; by Xunta de Galicia (Centro singular de investigación de Galicia accreditation 2019-2022), by European Union ERDF; and by Grant CEX2023-001318-M funded by MICIU/AEI/10.13039/501100011033 and by ERDF/EU. X. M. L.'s contribution to this work is also supported under scholarship No. PRE2021-097748, funded by MCIN/AEI/10.13039/501100011033 and FSE+. This work is also supported by the U.S. Department of Energy, Office of Science, Office of Nuclear Physics, within the framework of the Saturated Glue (SURGE) Topical Theory Collaboration.

[1] A. J. Larkoski, I. Moult, and B. Nachman, Jet substructure at the large hadron collider: A review of recent advances in theory and machine learning, Phys. Rep. **841**, 1 (2020).
[2] G. P. Salam, Towards jetography, Eur. Phys. J. C **67**, 637 (2010).
[3] S. Sapeta, QCD and jets at hadron colliders, Prog. Part. Nucl. Phys. **89**, 1 (2016).
[4] F. Gelis, E. Iancu, J. Jalilian-Marian, and R. Venugopalan, The color glass condensate, Annu. Rev. Nucl. Part. Sci. **60**, 463 (2010).
[5] A. Morreale and F. Salazar, Mining for gluon saturation at colliders, Universe **7**, 312 (2021).
[6] W. Busza, K. Rajagopal, and W. van der Schee, Heavy ion collisions: The big picture, and the big questions, Annu. Rev. Nucl. Part. Sci. **68**, 339 (2018).
[7] E. Craft, K. Lee, B. Meçaj, and I. Moult, Beautiful and charming energy correlators, arXiv:2210.09311.
[8] K. Lee, B. Meçaj, and I. Moult, Conformal colliders meet the LHC, Phys. Rev. D **111**, L011502 (2025).
[9] L. J. Dixon, I. Moult, and H. X. Zhu, Collinear limit of the energy-energy correlator, Phys. Rev. D **100**, 014009 (2019).
[10] I. Moult and H. X. Zhu, Simplicity from recoil: The three-loop soft function and factorization for the energy-energy correlation, J. High Energy Phys. 08 (2018) 160.
[11] Z.-B. Kang, J. Penttala, and C. Zhang, Determination of the strong coupling constant and the Collins-Soper kernel from the energy-energy correlator in e^+e^- collisions, arXiv:2410.21435.
[12] X. Liu and H. X. Zhu, Nucleon energy correlators, Phys. Rev. Lett. **130**, 091901 (2023).
[13] H. Chen, I. Moult, and H. X. Zhu, Quantum interference in jet substructure from spinning gluons, Phys. Rev. Lett. **126**, 112003 (2021).
[14] K. Lee and I. Moult, Energy correlators taking charge, arXiv:2308.00746.
[15] CMS Collaboration, Energy-energy correlators from PbPb and pp collisions at 5.02 TeV (2024), https://inspirehep.net/literature/2817909.
[16] A. Hayrapetyan *et al.* (CMS Collaboration), Measurement of energy correlators inside jets and determination of the strong coupling $\alpha_S(m_Z)$, Phys. Rev. Lett. **133**, 071903 (2024).
[17] S. Acharya *et al.* (ALICE Collaboration), Exposing the parton-hadron transition within jets with energy-energy correlators in pp collisions at $\sqrt{s} = 5.02$ TeV, arXiv:2409.12687.
[18] C. L. Basham, L. S. Brown, S. D. Ellis, and S. T. Love, Energy correlations in perturbative quantum chromodynamics: A conjecture for all orders, Phys. Lett. **85B**, 297 (1979).
[19] C. L. Basham, L. S. Brown, S. D. Ellis, and S. T. Love, Energy correlations in electron—positron annihilation: Testing QCD, Phys. Rev. Lett. **41**, 1585 (1978).
[20] D. M. Hofman and J. Maldacena, Conformal collider physics: Energy and charge correlations, J. High Energy Phys. 05 (2008) 012.
[21] N. A. Sveshnikov and F. V. Tkachov, Jets and quantum field theory, Phys. Lett. B **382**, 403 (1996).
[22] P. T. Komiske, I. Moult, J. Thaler, and H. X. Zhu, Analyzing N-point energy correlators inside jets with CMS open data, Phys. Rev. Lett. **130**, 051901 (2023).
[23] B. Singh and V. Vaidya, Factorization for energy-energy correlator in heavy ion collision, arXiv:2408.02753.
[24] J. Barata, P. Caucal, A. Soto-Ontoso, and R. Szafron, Advancing the understanding of energy-energy correlators in heavy-ion collisions, J. High Energy Phys. 11 (2024) 060.
[25] Z. Yang, Y. He, I. Moult, and X.-N. Wang, Probing the short-distance structure of the quark-gluon plasma with energy correlators, Phys. Rev. Lett. **132**, 011901 (2024).
[26] W.-J. Xing, S. Cao, G.-Y. Qin, and X.-N. Wang, Flavor hierarchy of jet energy correlators inside the quark-gluon plasma, Phys. Rev. Lett. **134**, 052301 (2025).

[27] J. Barata, J. G. Milhano, and A. V. Sadofyev, Picturing QCD jets in anisotropic matter: From jet shapes to energy correlators, Eur. Phys. J. C **84**, 174 (2024).

[28] K. Devereaux, W. Fan, W. Ke, K. Lee, and I. Moult, Imaging cold nuclear matter with energy correlators, arXiv:2303.08143.

[29] H. T. Li, I. Vitev, and Y. J. Zhu, Transverse-energy-energy correlations in deep inelastic scattering, J. High Energy Phys. 11 (2020) 051.

[30] H. T. Li, Y. Makris, and I. Vitev, Energy-energy correlators in deep inelastic scattering, Phys. Rev. D **103**, 094005 (2021).

[31] H.-Y. Liu, X. Liu, J.-C. Pan, F. Yuan, and H. X. Zhu, Nucleon energy correlators for the color glass condensate, Phys. Rev. Lett. **130**, 181901 (2023).

[32] H. Cao, X. Liu, and H. X. Zhu, Toward precision measurements of nucleon energy correlators in lepton-nucleon collisions, Phys. Rev. D **107**, 114008 (2023).

[33] X. L. Li, X. Liu, F. Yuan, and H. X. Zhu, Illuminating nucleon-gluon interference via calorimetric asymmetry, Phys. Rev. D **108**, L091502 (2023).

[34] H. Bossi, A. S. Kudinoor, I. Moult, D. Pablos, A. Rai, and K. Rajagopal, Imaging the wakes of jets with energy-energy-energy correlators, J. High Energy Phys. 12 (2024) 073.

[35] Y. Fu, B. Müller, and C. Sirimanna, Modification of the jet energy-energy correlator in cold nuclear matter, arXiv:2411.04866.

[36] C. Andres, F. Dominguez, R. Kunnawalkam Elayavalli, J. Holguin, C. Marquet, and I. Moult, Resolving the scales of the quark-gluon plasma with energy correlators, Phys. Rev. Lett. **130**, 262301 (2023).

[37] M. Jaarsma, Y. Li, I. Moult, W. J. Waalewijn, and H. X. Zhu, Energy correlators on tracks: Resummation and non-perturbative effects, J. High Energy Phys. 12 (2023) 087.

[38] J. C. Collins and D. E. Soper, Back-to-back jets in QCD: Comparison with experiment, Phys. Rev. Lett. **48**, 655 (1982).

[39] D. de Florian and M. Grazzini, The back-to-back region in e^+e^- energy-energy correlation, Nucl. Phys. **B704**, 387 (2005).

[40] Z. Tulipánt, A. Kardos, and G. Somogyi, Energy–energy correlation in electron–positron annihilation at NNLL + NNLO accuracy, Eur. Phys. J. C **77**, 749 (2017).

[41] A. Kardos, S. Kluth, G. Somogyi, Z. Tulipánt, and A. Verbytskyi, Precise determination of $\alpha_S(M_Z)$ from a global fit of energy–energy correlation to NNLO + NNLL predictions, Eur. Phys. J. C **78**, 498 (2018).

[42] X. Liu, W. Vogelsang, F. Yuan, and H. X. Zhu, Universality in the near-side energy-energy correlator, Phys. Rev. Lett. **134**, 151901 (2025).

[43] H.-y. Liu, K. Xie, Z. Kang, and X. Liu, Single inclusive jet production in pA collisions at NLO in the small-x regime, J. High Energy Phys. 07 (2022) 041.

[44] J. L. Albacete and C. Marquet, Single inclusive hadron production at RHIC and the LHC from the color glass condensate, Phys. Lett. B **687**, 174 (2010).

[45] E. Levin and A. H. Rezaeian, Gluon saturation and inclusive hadron production at LHC, Phys. Rev. D **82**, 014022 (2010).

[46] A. M. Staśto, B.-W. Xiao, F. Yuan, and D. Zaslavsky, Matching collinear and small x factorization calculations for inclusive hadron production in pA collisions, Phys. Rev. D **90**, 014047 (2014).

[47] J. P. Blaizot, F. Gelis, and R. Venugopalan, High-energy pA collisions in the color glass condensate approach. 1. Gluon production and the Cronin effect, Nucl. Phys. **A743**, 13 (2004).

[48] J. P. Blaizot, F. Gelis, and R. Venugopalan, High-energy pA collisions in the color glass condensate approach. 2. Quark production, Nucl. Phys. **A743**, 57 (2004).

[49] M. Bury, H. Van Haevermaet, A. Van Hameren, P. Van Mechelen, K. Kutak, and M. Serino, Single inclusive jet production and the nuclear modification ratio at very forward rapidity in proton-lead collisions with $\sqrt{s_{NN}} =$ 5.02 TeV, Phys. Lett. B **780**, 185 (2018).

[50] A. Dumitru, A. Hayashigaki, and J. Jalilian-Marian, The color glass condensate and hadron production in the forward region, Nucl. Phys. **A765**, 464 (2006).

[51] H.-Y. Liu, Y.-Q. Ma, and K.-T. Chao, Improvement for color glass condensate factorization: Single hadron production in pA collisions at next-to-leading order, Phys. Rev. D **100**, 071503 (2019).

[52] Y. Guo, X. Liu, and F. Yuan, Long range energy-energy correlator at the LHC, arXiv:2408.14693.

[53] J. C. Collins, D. E. Soper, and G. F. Sterman, Factorization of hard processes in QCD, Adv. Ser. Dir. High Energy Phys. **5**, 1 (1989).

[54] G. T. Bodwin, Factorization of the Drell-Yan cross-section in perturbation theory, Phys. Rev. D **31**, 2616 (1985); **34**, 3932(E) (1986).

[55] J. C. Collins, D. E. Soper, and G. F. Sterman, Soft gluons and factorization, Nucl. Phys. **B308**, 833 (1988).

[56] J. Collins, Foundations of Perturbative QCD, *Vol. 32 of Cambridge Monographs on Particle Physics*, Nuclear Physics and Cosmology (Cambridge University Press, Cambridge, England, 2023).

[57] J. F. Owens, Large momentum transfer production of direct photons, jets, and particles, Rev. Mod. Phys. **59**, 465 (1987).

[58] Z.-B. Kang, F. Ringer, and I. Vitev, The semi-inclusive jet function in SCET and small radius resummation for inclusive jet production, J. High Energy Phys. 10 (2016) 125.

[59] Z.-B. Kang, K. Lee, X. Liu, and F. Ringer, Soft drop groomed jet angularities at the LHC, Phys. Lett. B **793**, 41 (2019).

[60] K. Lee, I. Moult, and X. Zhang, Revisiting single inclusive jet production: Timelike factorization and reciprocity, J. High Energy Phys. 05 (2025) 129.

[61] See Supplemental Material at http://link.aps.org/supplemental/10.1103/96xh-bd1w for the evolution of the jet function in position space and for the medium modification factors.

[62] J. C. Collins, D. E. Soper, and G. F. Sterman, Transverse momentum distribution in Drell-Yan pair and W and Z boson production, Nucl. Phys. **B250**, 199 (1985).

[63] J. Collins and T. Rogers, Understanding the large-distance behavior of transverse-momentum-dependent parton densities and the Collins-Soper evolution kernel, Phys. Rev. D **91**, 074020 (2015).

[64] Z.-B. Kang, X. Liu, F. Ringer, and H. Xing, The transverse momentum distribution of hadrons within jets, J. High Energy Phys. 11 (2017) 068.

[65] T.-J. Hou *et al.*, Progress in the CTEQ-TEA NNLO global QCD analysis, arXiv:1908.11394.
[66] B. Jacak (private communication).
[67] J. H. Isaksen and K. Tywoniuk, Wilson line correlators beyond the large-N_c, J. High Energy Phys. 11 (2020) 125.
[68] J. H. Isaksen and K. Tywoniuk, Precise description of medium-induced emissions, J. High Energy Phys. 09 (2023) 049.
[69] L. Apolinário, N. Armesto, J. G. Milhano, and C. A. Salgado, Medium-induced gluon radiation and colour decoherence beyond the soft approximation, J. High Energy Phys. 02 (2015) 119.
[70] A. Kovner and U. A. Wiedemann, Eikonal evolution and gluon radiation, Phys. Rev. D **64**, 114002 (2001).
[71] T. Altinoluk, N. Armesto, G. Beuf, M. Martínez, and C. A. Salgado, Next-to-eikonal corrections in the CGC: Gluon production and spin asymmetries in pA collisions, J. High Energy Phys. 07 (2014) 068.
[72] J. Barata, C. A. Salgado, and J. M. Silva, Gluon to $q\bar{q}$ antenna in anisotropic QCD matter: Spin-polarized and azimuthal jet observables, J. High Energy Phys. 12 (2024) 023.
[73] M. Attems, J. Brewer, G. M. Innocenti, A. Mazeliauskas, S. Park, W. van der Schee, and U. A. Wiedemann, The medium-modified $g \to c\bar{c}$ splitting function in the BDMPS-Z formalism, J. High Energy Phys. 01 (2023) 080.
[74] Y.-Y. Zhang and X.-N. Wang, Parton rescattering and gluon saturation in dijet production at EIC, Phys. Rev. D **105**, 034015 (2022).
[75] P. Ru, Z.-B. Kang, E. Wang, H. Xing, and B.-W. Zhang, Global extraction of the jet transport coefficient in cold nuclear matter, Phys. Rev. D **103**, L031901 (2021).
[76] K. J. Eskola, P. Paakkinen, H. Paukkunen, and C. A. Salgado, EPPS21: A global QCD analysis of nuclear PDFs, Eur. Phys. J. C **82**, 413 (2022).
[77] A. Nambrath, Energy-energy correlators of inclusive jets from small to large collision systems with the ALICE experiment, Presented at Hard Probes 2024, Nagasaki, Japan, 2024, https://indico.cern.ch/event/1339555/contributions/6040810/attachments/2932582/5150292/HP24_ALICE_EECs.pdf.
[78] J. Barata, M. V. Kuzmin, J. G. Milhano, and A. V. Sadofyev, Jet EEC aWAKEning: Hydrodynamic response on the celestial sphere, https://inspirehep.net/literature/2856224.